Ligand-responsive RNA mechanical switches

Mark A Boerneke & Thomas Hermann

Ligand-responsive RNA mechanical switches

Mark A Boerneke[1] and Thomas Hermann[1,2,*]

[1]Department of Chemistry and Biochemistry; University of California, San Diego; La Jolla, CA USA; [2]Center for Drug Discovery Innovation; University of California, San Diego; La Jolla, CA USA

Ligand-responsive RNA mechanical switches represent a new class of simple switching modules that adopt well-defined ligand-free and bound conformational states, distinguishing them from metabolite-sensing riboswitches. Initially discovered in the internal ribosome entry site (IRES) of hepatitis C virus (HCV), these RNA switch motifs were found in the genome of diverse other viruses. Although large variations are seen in sequence and local secondary structure of the switches, their function in viral translation initiation that requires selective ligand recognition is conserved. We recently determined the crystal structure of an RNA switch from Seneca Valley virus (SVV) which is able to functionally replace the switch of HCV. The switches from both viruses recognize identical cognate ligands despite their sequence dissimilarity. Here, we describe the discovery of 7 new switches in addition to the previously established 5 examples. We highlight structural and functional features unique to this class of ligand-responsive RNA mechanical switches and discuss implications for therapeutic development and the construction of RNA nanostructures.

Ligand-Responsive RNA Mechanical Switches Versus Metabolite-Sensing Riboswitches

Over the course of the last decades, structural and functional studies have expanded our understanding of the numerous roles that RNA plays in addition to transferring genetic information from DNA into proteins, including its ability to regulate diverse cellular processes.[1] Many of these roles involve a switching transformation between 2 different structural states of an RNA each of which exerts a distinct function. The most common of these switches are known as riboswitches which act as genetic regulatory on-off switches in mRNA by directly binding small molecule metabolites. The binding of a ligand to a riboswitch sensor domain induces secondary structure changes within a second domain, the expression platform, which regulates downstream transcription and translation of the mRNA (**Fig. 1A**). Exhaustive rearrangement of base pairs in the switching sequence results in different secondary structures of riboswitches in the presence or absence of a binding ligand.[2-4]

Unlike riboswitches, the RNA switches described here are unique in their small size (**Fig. 1B**) and mechanical responsiveness to ligand binding which gives rise to 2 distinct and stable conformational states implicated with a switching function during viral translation initiation[5] (**Fig. 1C**). The viral RNA switches adopt an L-shaped conformation stabilized by magnesium ions (**Fig. 2A**, **Fig. 3A**) or cross-over base pairing (**Fig. 3B**), and are captured in a straightened conformation by ligands binding in a deep pocket[5–12] (**Fig. 2B**, **Fig. 4**). The individual conformational states interconvert as a result of the rearrangement of magnesium ions and unpaired bases in the internal loop RNA, and without breaking or new formation of any base pairs in the secondary structure as occurs in riboswitches. The requirement for 2 stable switch conformations where each internal loop base has specific functional interactions in both the ligand-bound and unbound structural state leads to the high level of sequence conservation seen in virus clinical isolates.[8,9] Conformational dynamics of the switches is
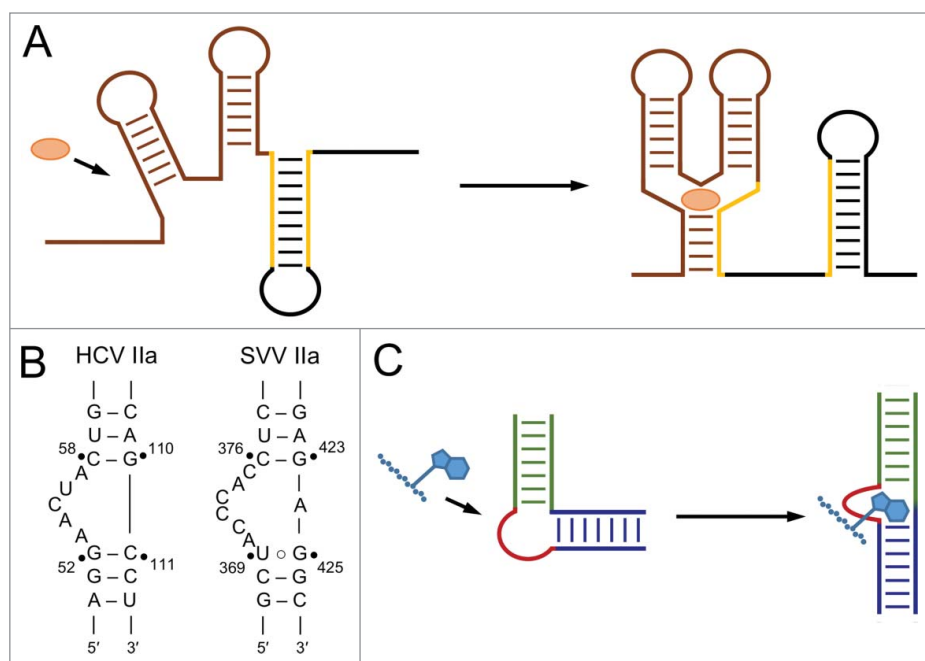
Figure 1. Comparison of ligand-responsive RNA mechanical switches in contrast to metabolite-sensing riboswitches. (**A**) Metabolite-sensing riboswitches consist of a sensor domain (brown) linked to an expression platform (yellow and black) and exist in structurally diverse metabolite-free or bound conformations. The binding of a metabolite (orange) induces structural changes to the RNA switching sequence (yellow), resulting in folding and base-pairing patterns that are distinct from the metabolite-free conformation. (**B**) Predicted secondary structure for HCV and SVV IIa RNA switches. (**C**) Ligand-responsive RNA mechanical switches are composed of a small internal loop (red) of 3–6 unpaired bases and 2 flanking helices (green and dark blue) of double stranded RNA and adopt distinct ligand-free (bent) and ligand-captured (elongated) conformations. The ligand-free bent conformation is stabilized by magnesium ions (not shown) and continuous stacking interactions of unpaired bases in the internal loop. Ligand (light blue) binding captures the elongated conformation of the RNA in a process that involves rearrangement of magnesium ions and unpaired bases but does not affect the integrity of base pairs of the flanking helices.
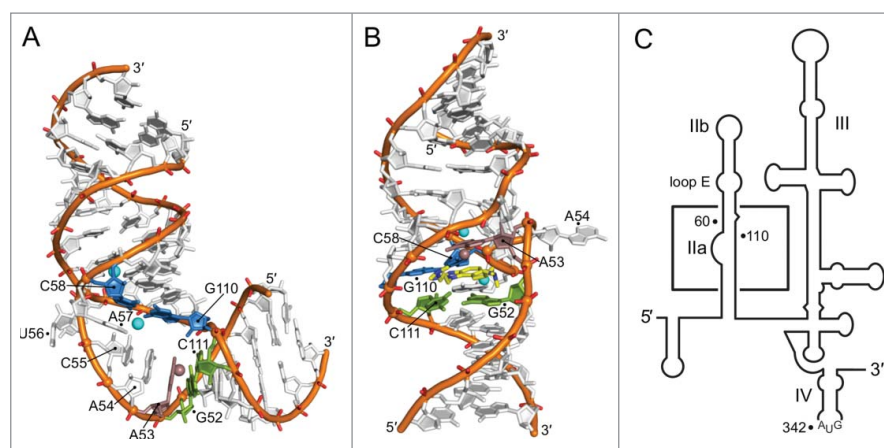

Figure 2. Structure of HCV IRES subdomain IIa RNA switch in absence and presence of binding ligand. Colors of highlighted bases are described in **Figure 3**. (**A**) Crystal structure of ligand-free IIa RNA switch from HCV shown with stabilizing magnesium ions and flanking helices adopting a bent conformation. (**B**) Crystal structure of ligand-captured IIa RNA switch from HCV adopting an elongated conformation. (**C**) Secondary structure of the HCV IRES element in the 5′ untranslated region of the viral genome. Subdomain IIa is highlighted inside a box.

required for biological function as capture in one of the individual states by synthetic inhibitor binding inactivates the switch.[9] These switches do not undergo secondary structure changes but rather a simple mechanical switching between 2 distinct and stable conformations that are required as functional states during translation initiation, similar to a light switch whose moving parts translocate and rotate but do not undergo reassembly during actuation.

Discovery of the RNA Switches in Viral IRES Elements

The archetype of these switches was discovered in the internal ribosome entry site (IRES) of hepatitis C virus (HCV). The 5′ untranslated region of some eukaryotic and viral mRNAs contains a structured IRES element that initiates translation by assembling functional ribosomes directly at the start codon and bypassing the need for 5′ cap recognition, ribosome scanning, as well as the requirement for most initiation factors.[13-16] Within the HCV IRES, which is composed of several domains (**Fig. 2C**), domain II is highly conserved in thousands of clinical isolates[7-9] and contains an internal loop in its lower stem, subdomain IIa (**Fig. 2C**), which is the target for viral translation inhibitors.[17] The three dimensional structure of subdomain IIa was determined by x-ray crystallography[6] (**Fig. 2A**, **Fig. 3A**), which revealed the RNA adopting a 90° bent architecture, in agreement with cryo-EM and NMR studies.[18-20] FRET experiments demonstrated that the subdomain IIa undergoes a conformational switch in the presence of benzimidazole viral translation inhibitors.[7,17] The co-crystal structure of subdomain IIa in complex with benzimidazole inhibitor **1** showed capture of the RNA in an extended conformation[8] (**Fig. 2B**, **Fig. 4**). We recently demonstrated that the ligand pocket in subdomain IIa selectively recognizes guanine and serves as a fortuitous binding site for structurally similar benzimidazoles. Based on this observation in conjunction with other circumstantial evidence,[21] we hypothesized that a guanosine within an
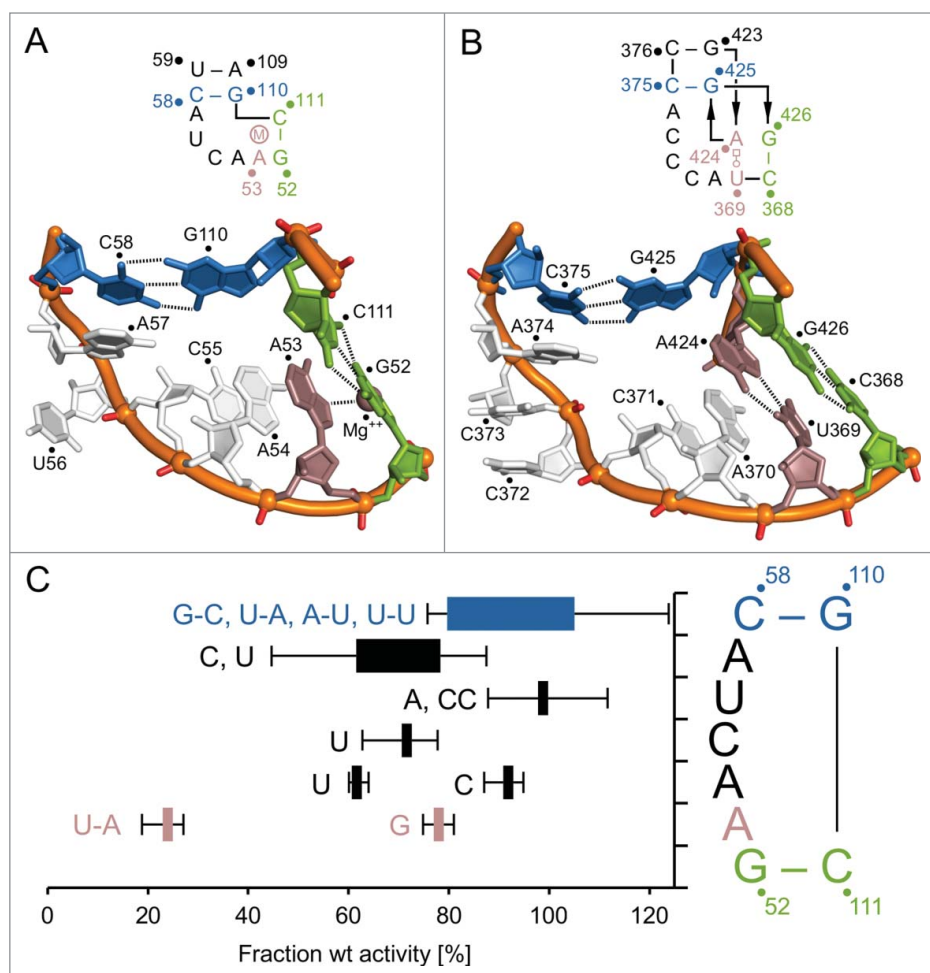
Figure 3. Structures of IRES subdomain IIa RNA switches from SVV and HCV. Colors highlight corresponding elements in each switch. (**A**) Secondary structure schematic and crystal structure of HCV IIa highlighting closing base pairs (top-blue; bottom-green) and A53 stabilized by a magnesium ion (mauve,) that occupies a similar space as the U◯A Hoogsteen pair in the SVV motif. (**B**) Secondary structure schematic and crystal structure of SVV IIa highlighting closing base pairs (top-blue; bottom-green) and unusual U◯A Hoogsteen pair (mauve). Local inversion of strand directionality is indicated by arrows. (**C**) Mutational analysis of HCV IIa switch activity studied in the context of an in vitro translation (IVT) assay. Box width indicates the range of average activity for each mutation as a percent of wild type activity. Error bars indicate minimum and maximum observed values for each set of mutations.

RNA sequence of the viral genome or rRNA acts as a trigger of the IIa conformational switch.[5]

A number of other viruses in the flavivirus and picornavirus families also contain HCV-like IRES elements with varying degrees of structural and functional similarity but only limited sequence conservation.[5,22] Despite the differences, most IRES elements are organized into similar domains and contain analogous domain II elements, 12 of which will be discussed here. The subdomain IIb

hairpin loop and internal loop E motifs (**Fig. 2C**) are conserved in HCV, CSFV, BVDV, AEV, BDV, NPHV, and GPV while SVV, SPV, DPV, GBV, and DHV maintain sequence conservation of their loop E motif but not the IIb hairpin loop. All twelve of these viruses contain a subdomain IIa internal loop switch structure in the 5′- or 3′-proximal strand of the lower domain II stem. The switch motifs range in size from 9–12 bases, 3 to 6 of which are unpaired, and display little to no sequence conservation[5] (**Fig. 5**).

Structure of the Ligand-Free RNA Switches in HCV and SVV

Sequence and structure analyses of HCV-like IRES elements have allowed us to develop consensus models of domain II secondary structure and subdomain IIa switch motifs. X-ray crystallography has been used to determine the 3-dimensional structure of the HCV and SVV switches in the ligand-free state[5,6] and the HCV switch in complex with a viral translation inhibitor ligand. The CSFV switch has been characterized by NMR spectroscopy.[23]

While HCV and SVV IIa switches have quite different sequences and predicted secondary structures (**Fig. 1A**), their overall 3 dimensional structures, as determined by x-ray crystallography, are almost identical[5,7] (**Fig. 3A, B**). Both switches have a C-G pair (blue, **Fig. 3**) closing the internal loop at the upper flanking helix. For SVV, this C-G pair is formed by G425 from the 3′-proximal side of the IIa stem, crossing over and forming a Watson-Crick base pair with C375, which diverges from the predicted secondary structure (**Fig. 1B**) and inverts local strand directionality between G423 and G426 (**Fig. 3B**). The IIa switches from both HCV and SVV share an A base (A57 in HCV, A374 in SVV) stacking beneath the C (C58 in HCV, C375 in SVV) of the closing base pair. In SVV, 2 C residues (C373, C372) stack beneath A374, while in HCV, a single U base (U56) fills this same space and packs against the ribose of A57. This upper part of the switch, including half of the IIa internal loop and the flanking upper helix, is oriented at a 90° angle relative to the lower helix which connects through perpendicularly arranged bases of the lower IIa loop. The G52-C111 Watson-Crick pair closes the bottom of the internal loop in HCV, and corresponds to the C368-G426 pair in SVV (green, **Fig. 3**). Stacking above the C368-G426 pair in SVV, a reverse Hoogsteen pair U369◯A424 forms in which the Watson-Crick edge of U369 pairs with the Hoogsteen edge of A424 (mauve, **Fig. 3B**). In HCV, this space is occupied by A53 which interacts with a magnesium
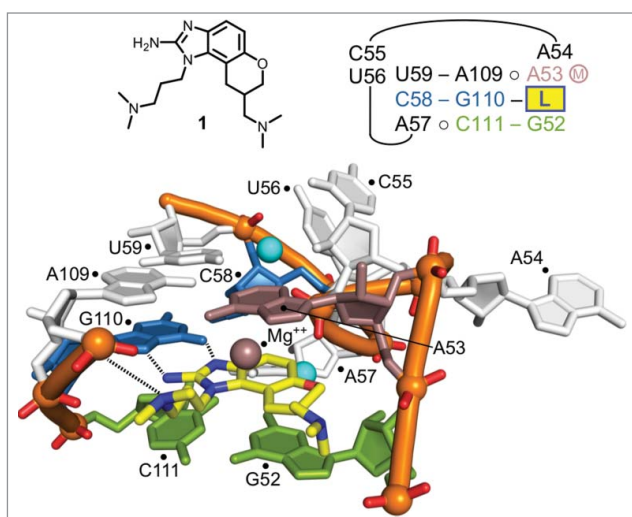
Figure 4. Structure of the HCV IRES subdomain IIa RNA switch in complex with ligand 1. The color scheme is identical to **Figure 2** with the addition of ligand 1 in yellow and 2 additional magnesium ions (cyan). When the HCV IIa switch is bound by ligand 1, closing base pairs (blue and green) and adjacent helices maintain Watson-Crick base pairing. Rearrangement of unpaired internal loop bases and magnesium ions occurs to form a deep ligand-binding pocket. The roof of the binding pocket involves the U59-A109◯A53 base triple, while the floor is formed by the A57◯C111-G52 triple. The guanidinium ion-like moiety of ligand 1 interacts with the Hoogsteen edge of G110 forming a C58-G110◯Ligand pseudo-base triple-like complex. The phosphate of U56 is shown coordinated to 2 magnesium ions (cyan). Secondary structure schematic indicates the stacking of these 3 base triples, and the flipped out bases U56, C55, and A54.

ion (mauve, **Fig. 3A**) and stacks above the G52-C111 closing pair. Two bases (A54, C55) stack above A53 in HCV, which correspond to A370 and C371 stacking above U369 in SVV. All unpaired bases in the IIa motifs from both viruses stack continuously on either of the flanking helices with the exception of U56 in HCV whose stacking interaction may be interrupted by crystal packing, and is seen stacking in some solution conformations observed by NMR.[20] The folds of both the SVV and HCV switch motifs are unprecedented in other RNA architectures. Part of the SVV motif (C368-G426, G425, and U369◯A424) resembles a UA-handle which is found as a recurring minimal building block in numerous other RNA architectures.[24-25] Systematic mutational analyses of residues in the HCV subdomain IIa reveal that some structural sites tolerate change while others do not, generally in agreement with interactions observed for these residues in the crystal structure (**Fig. 3C**). Consequently, certain combinations of multiple mutations lead to functionally fit switches while the constituting individual base changes may cause reduction in translation activity (**Fig. 5**).
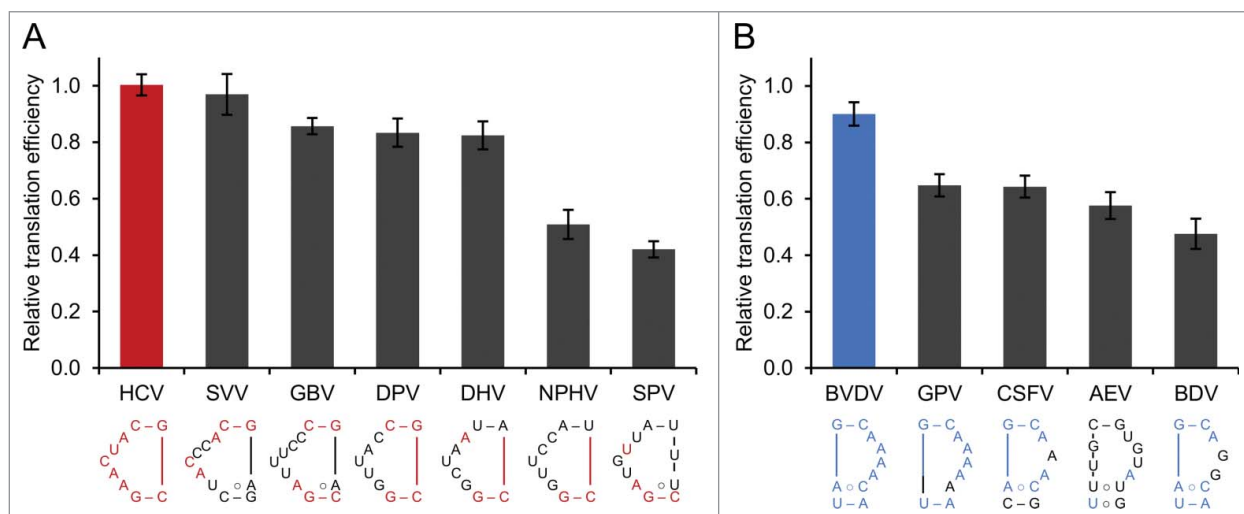

Figure 5. Functional activity and secondary structures of IRES IIa switches. (**A**) In vitro translation activity of HCV IRES chimeras with subdomain IIa replacement by corresponding HCV-like viral IRES IIa elements. Sequences conserved with HCV are shown in red. Secondary structure for SVV is drawn to indicate how bases overlay with HCV in 3-dimensional space as seen in the crystal structures. Other IIa element secondary structures are drawn as predicted to overlay with HCV IIa. (**B**) In vitro translation activity of HCV IRES chimeras with domain II replacement with BVDV and subdomain IIa replacement by corresponding BVDV-like viral IRES IIa elements. Values were normalized to HCV wt. Sequences conserved with BVDV are shown in blue. IIa element secondary structures are drawn as predicted to overlay with BVDV IIa. NCBI reference sequences: HCV (NC_004102), SVV (NC_011349.1), GBV (NC_001655.1), DPV (AY563023.1), DHV (DQ249299.1), NPHV (JQ434001.1), SPV (AY064717.2), BVDV (NC_001461.1), GPV (NC_003678.1), CSFV (NC_002657.1), AEV (NC_003990.1), BDV (NC_003679.1).

Structure of a Ligand-Bound Switch

X-ray crystal structure analysis of the HCV IIa switch in complex with a viral translation inhibitor ligand revealed an elongated conformation of the RNA which maintains all base pairs seen in the bent conformation.[8] A deep ligand binding pocket is formed by the rearrangement of magnesium ions and unpaired internal loop bases to form additional base triple interactions. The roof of the binding pocket is formed by base triple U59-A109○A53 with the Watson-Crick edge of A53 pairing to the Hoogsteen edge of A109. The N7 atom of A53 is coordinated to a magnesium ion, unchanged from the ligand-free state of the RNA (mauve, **Fig. 4**). The U59-A109 pair remains stacked above the C58-G110 pair as it does in the ligand-free state (not shown in **Fig. 3B**). A53 stacks above the binding ligand (yellow, **Fig. 4**) which engages in a pseudo-base triple interaction with C58-G110 (blue, **Fig. 4**). The Hoogsteen edge of G110 recognizes the guanidinium cation-like moiety of the amino-benzimidazole ligand. The floor of the binding pocket is formed by base triple A57○C111-G52, with G52 stacking beneath the ligand, and the sugar edge of C111 (green, **Fig. 4**) pairing with the Watson-Crick edge of A57. U56, C55, and A54 are all flipped out of the helix with U56 and C55 stacking onto each other. The phosphate group of U56 is rotated into the back of the ligand-binding pocket, where it coordinates 2 magnesium ions (cyan, **Fig. 4**). One of the metal ions interacts with U59 in the roof of the binding pocket while the other is coordinated to A57 in the floor. An additional hydrogen bonding interaction occurs between the protonated dimethylamino propyl side chain of the ligand and the phosphate group of A109.

IIa Switch Function

IIa RNA switch motifs have been shown to facilitate viral translation initiation by assuming bent and elongated conformations, and directing the IIb hairpin to the E-site at the ribosomal subunit interface.[5,18,19] We recently demonstrated that switching between bent and elongated conformations occurs in IIa switches from diverse viruses including HCV, BVDV, CSFV, SVV, and AEV by FRET.[5,7] Additionally, IIa switch functionality in initiating HCV IRES translation has been demonstrated using an in vitro translation (IVT) assay and replicon-transfected human cells.[5] HCV chimeric IVT reporter constructs obtained by replacing HCV whole domain II with analogous domains from BVDV, CSFV, or AEV yield IRESs proficient in initiating translation, with BVDV domain II displaying near wild-type activity[5] (blue, **Fig. 5B**). Replacement of the HCV subdomain IIa switch only with the analogous motif from SVV, guided by x-ray crystal structures, furnished a fully functional IRES both in an in vitro translation and HCV replicon assay, despite only marginal sequence similarity shared between the viral IIa motifs[5] (**Figs. 1B and 5A**). These experiments established the distinct viral RNA IIa motifs as minimal architectural switch modules participating in a conserved biological function. Inspired by these findings, we set out to search for similar switch motifs in other viruses. Guided by a consensus secondary structure model for HCV domain II-like fragments, we identified 7 new distinct switches in addition to those from HCV, SVV, BVDV, CSFV, and AEV. The new switches were found in the viral IRES elements of GBV, DPV, DHV, NPHV, SPV, GPV, and BDV. All switches, in addition to those from HCV and SVV, demonstrated proficiency in translation initiation when tested in the context of HCV IRES chimeras in the IVT assay (**Fig. 5**). IIa switches with an internal loop occurring in the 5′ proximal strand of the lower domain II stem were deemed to be HCV-like and were used to replace the HCV subdomain IIa in the chimeric IVT reporter construct as described above for SVV (**Fig. 5A**). IIa switches with an internal loop in the 3′ proximal strand of the lower domain II stem were deemed to be BVDV-like and were used to replace the BVDV subdomain IIa in the HCV/BVDV domain II chimeric IVT reporter construct as described above (**Fig. 5B**). IIa switch sequences used to replace respective HCV or BVDV switches are shown in **Figure 5**. The modular nature of these distinct switches suggests that they have adapted in their different viral contexts to perform corresponding biological functions. It has been suggested that IRES architectures may have been exchanged between viral genomes by horizontal transfer and multiple recombination events.[22] Transfer of IRES elements has been observed within viral families and may also occur between families and through capture of cellular RNA elements.[22] Widely divergent switches, such as those involving variation of the internal loop motif occurring in the 3′ versus 5′ proximal strand of the lower domain II stem, in distinct viral families, may also have originated from repeated adaptation of independently evolving motifs that eventually converged to provide similar functions.

Significance and Applications of the IIa Switches

The IRES subdomain IIa switch has been exploited as a therapeutic target to selectively suppress viral translation with synthetic inhibitors that capture specific conformations of the RNA.[5,7,9-12] High levels of conservation in HCV clinical isolates and the presence of a deep solvent-excluded ligand binding pocket render the IIa RNA switch a target for the development of antiviral drugs. In the context of viral IRES function, the IIa switches are involved in the dynamic interplay of ribosomal subunit recruitment and the transitioning from translation initiation to elongation,[18-19,23,26-31] which are facilitated by transient interaction with a G residue that captures a conformational change in the IIa RNA.[5]

It is conceivable that similar ligand-responsive switches occur in other non-coding RNAs to regulate interactions with nucleic acid or protein partners. Mechanical switches that do not undergo global changes in secondary structure, involving the kinetically slow disruption and formation of base pairs as is common in riboswitches, may be preferred for transient regulatory or pausing events that are quickly reversible. While the dynamics of

IRES binding and ribosome release during initiation is not yet fully understood, it has been observed that ribosomes stall on the IRES in the presence of IIa-targeting inhibitor ligands or when the IIa switch is deleted.[9,23,29] Ligand-responsive mechanical switches provide a simple mechanism to regulate binding and release events of RNA-RNA and RNA-protein interactions contingent on the presence of a trigger ligand.

The IIa RNA switch motifs have also been exploited as rectangular building blocks to rationally design and construct nanostructures with a variety of potential applications. We used the HCV IIa switch to build a self-assembling RNA square that adopts a well-defined structure as revealed by X-ray structure analysis.[32] Recently, the same RNA switch has been incorporated into a self-assembling nanoprism.[33] Other RNA switches, including the previously discovered SVV subdomain IIa[5] and the IIa-like viral motifs described here, provide a growing tool box of bent RNA motifs to use as building blocks for complex RNA nanostructures that self-assemble from short oligonucleotides and have the potential to change conformation in response to selective ligand binding.

Conclusions

In conclusion, we have described what are currently the simplest known ligand-dependent mechanical switching motifs found in noncoding RNA architectures. The HCV IIa switch has been characterized by x-ray crystallography for both the ligand-free and ligand-bound conformation. The crystal structure of a functionally analogous IIa switch from SVV in its ligand-free conformation was described, revealing a structural and functional interchangeability with the archetypical HCV switch despite a lack of sequence conservation. In addition to HCV and SVV, IIa-like RNA switches were discovered in 10 other viruses and were able to functionally replace the HCV IIa switch to create translationally competent IRES elements. These switches contain a recognition site for a guanosine residue and are fortuitous targets for synthetic viral translation inhibitors. Unlike metabolite-sensing

riboswitches, these ligand-responsive mechanical switches represent a new class of simple RNA modules that are structurally well-defined in both ligand-free and bound states despite their small size. The viral subdomain IIa-like modules may represent the simplest form of ligand-responsive mechanical switches in nucleic acids. While functioning in a dynamic fashion during viral translation initiation and elongation, these RNA motifs represent a unique therapeutic target as well as well-defined ligand-responsive building blocks for the construction of RNA nanostructures.

Disclosure of Potential Conflicts of Interest

No potential conflicts of interest were disclosed.

Funding

References

1. Cech TR, Steitz JA. The noncoding RNA revolution-trashing old rules to forge new ones. Cell 2014; 157:77–94; PMID:24679528; http://dx.doi.org/10.1016/j.cell.2014.03.008

2. Serganov A, Nudler E. A decade of riboswitches. Cell 2013; 152:17–24; PMID:23332744; http://dx.doi.org/10.1016/j.cell.2012.12.024

3. Garst AD, Edwards AL, Batey RT. Riboswitches: structures and mechanisms. Cold Spring Harb Perspect Biol 2011; 3:a003533; PMID:20943759

4. Roth A, Breaker RR. The Structural and Functional Diversity of Metabolite-Binding Riboswitches. Annu Rev Biochem 2009; 78:305–34; PMID:19298181; http://dx.doi.org/10.1146/annurev.biochem.78.070507.135656

5. Boerneke MA, Dibrov SM, Gu J, Wyles DL, Hermann T. Functional conservation despite structural divergence in ligand-responsive RNA switches. Proc Natl Acad Sci USA 2014; 111:15952–7; PMID:25349403; http://dx.doi.org/10.1073/pnas.1414678111

6. Dibrov SM, Johnston-Cox H, Weng Y-H, Hermann T. Functional architecture of HCV IRES domain II stabilized by divalent metal ions in the crystal and in solution. Angew Chem Int Ed Engl 2007; 46:226–9; PMID:17131443; http://dx.doi.org/10.1002/anie.200603807

7. Parsons J, Castaldi MP, Dutta S, Dibrov SM, Wyles DL, Hermann T. Conformational inhibition of the hepatitis C virus internal ribosome entry site RNA. Nat

Chem Biol 2009; 5:823–5; PMID:19767736; http://dx.doi.org/10.1038/nchembio.217

8. Dibrov SM, Ding K, Brunn ND, Parker MA, Bergdahl BM, Wyles DL, Hermann T. Structure of a hepatitis C virus RNA domain in complex with a translation inhibitor reveals a binding mode reminiscent of riboswitches. Proc Natl Acad Sci USA 2012; 109:5223–8; PMID:22431596; http://dx.doi.org/10.1073/pnas.1118699109

9. Dibrov SM, Parsons J, Carnevali M, Zhou S, Rynearson KD, Ding K, Garcia Sega E, Brunn ND, Boerneke MA, Castaldi MP, et al. Hepatitis C Virus Translation Inhibitors Targeting the Internal Ribosomal Entry Site. J Med Chem 2014; 57:1694–707; PMID:24138284; http://dx.doi.org/10.1021/jm401312n

10. Rynearson KD, Charrette B, Gabriel C, Moreno J, Boerneke MA, Dibrov SM, Hermann T. Two-Amino-benzoxazole ligands of the hepatitis C virus internal ribosome entry site. Bioorg Med Chem Lett 2014; 24:3521–25; PMID:24930829; http://dx.doi.org/10.1016/j.bmcl.2014.05.088

11. Ding K, Wang A, Boerneke MA, Dibrov SM, Hermann T. Aryl-substituted aminobenzimidazoles targeting the hepatitis C virus internal ribosome entry site. Bioorg Med Chem Lett 2014; 24:3113–7; PMID:24856063; http://dx.doi.org/10.1016/j.bmcl.2014.05.009

12. Carnevali M, Parsons J, Wyles DL, Hermann T. A modular approach to synthetic RNA binders of the hepatitis C virus internal ribosome entry site. Chembiochem 2010; 11:1364–7; PMID:20564282; http://dx.doi.org/10.1002/cbic.201000177

13. Plank T-DM, Kieft JS. The structures of nonprotein-coding RNAs that drive internal ribosome entry site function. Wiley Interdiscip. Rev. RNA 2012; 3:195–212; PMID:22215521

14. Hellen CUT, Pestova TV. Translation of hepatitis C virus RNA. J Viral Hepat 1999; 6:79–87; PMID:10607219; http://dx.doi.org/10.1046/j.1365-2893.1999.00150.x

15. Ji H, Fraser CS, Yu Y, Leary J, Doudna JA. Coordinated assembly of human translation initiation complexes by the hepatitis C virus internal ribosome entry site RNA. Proc Natl Acad Sci USA 2004; 101:16990–5

16. Otto GA, Puglisi JD. The Pathway of HCV IRES-Mediated Translation Initiation. Cell 2004; 119:369–80; PMID:15507208; http://dx.doi.org/10.1016/j.cell.2004.09.038

17. Seth PP, Miyaji A, Jefferson EA, Sannes-Lowery KA, Osgood SA, Propp SS, Ranken R, Massire C, Sampath R, Ecker DJ, et al. SAR by MS: discovery of a new class of RNA-binding small molecules for the hepatitis C virus: Internal ribosome entry site IIA subdomain. J Med Chem 2005; 48:7099–102; PMID:16279767; http://dx.doi.org/10.1021/jm050815o

18. Spahn CM, Kieft JS, Grassucci RA, Penczek PA, Zhou K, Doudna JA, Frank J. Hepatitis C virus IRES RNA-induced changes in the conformation of the 40s ribosomal subunit. Science 2001; 291:1959–62; PMID:11239155; http://dx.doi.org/10.1126/science.1058409

19. Boehringer D, Thermann R, Ostareck-Lederer A, Lewis JD, Stark H. Structure of the hepatitis C virus IRES bound to the human 80S ribosome: Remodeling of the HCV IRES. Structure 2005; 13:1695–706; PMID:16271893; http://dx.doi.org/10.1016/j.str.2005.08.008

20. Lukavsky P, Kim I, Otto G, Puglisi J. Structure of HCV IRES domain II determined by NMR. Nat Struct Biol 2003; 10:1033–8; PMID:14578934; http://dx.doi.org/10.1038/nsb1004

21. Berry KE, Waghray S, Mortimer SA, Bai Y, Doudna JA. Crystal structure of the HCV IRES central domain reveals strategy for start-codon positioning. Structure 2011; 19:1456–66; PMID:22000514; http://dx.doi.org/10.1016/j.str.2011.08.002

22. Hellen CUT, de Breyne S. A distinct group of hepacivirus/pestivirus-like internal ribosomal entry sites in members of

diverse picornavirus genera: evidence for modular exchange of functional noncoding RNA elements by recombination. J Virol 2007; 81:5850–63; PMID:17392358; http://dx.doi.org/10.1128/JVI.02403-06

23. Locker N, Easton L, Lukavsky P. HCV and CSFV IRES domain II mediate eIF2 release during 80S ribosome assembly. EMBO J 2007; 26:795–805; PMID:17255934; http://dx.doi.org/10.1038/sj.emboj.7601549

24. Jaeger L, Verzemnieks EJ, Geary C. The UA_handle: a versatile submotif in stable RNA architectures. Nucleic Acids Res 2009; 37:215–30; PMID:19036788; http://dx.doi.org/10.1093/nar/gkn911

25. Wadley LM, Pyle AM. The identification of novel RNA structural motifs using COMPADRES: an automated approach to structural discovery. Nucleic Acids Res 2004; 32:6650–9; PMID:15608296; http://dx.doi.org/10.1093/nar/gkh1002

26. Pestova TV, Shatsky IN, Fletcher SP, Jackson RJ, Hellen CUT. A prokaryotic-like mode of cytoplasmic eukaryotic ribosome binding to the initiation codon during internal translation initiation of hepatitis C and classical swine fever virus RNAs. Genes Dev 1998; 12:67–83; PMID:9420332; http://dx.doi.org/10.1101/gad.12.1.67

27. Kolupaeva VG, Pestova TV, Hellen CU. Ribosomal binding to the internal ribosomal entry site of classical swine fever virus. RNA 2000; 6:1791–807; PMID:11142379; http://dx.doi.org/10.1017/S1355838200000662

28. Filbin ME, Kieft JS. HCV IRES domain IIb affects the configuration of coding RNA in the 40S subunit's decoding groove. RNA 2011; 17:1258–73; PMID:21606179; http://dx.doi.org/10.1261/rna.2594011

29. Filbin ME, Vollmar BS, Shi D, Gonen T, Kieft JS. HCV IRES manipulates the ribosome to promote the switch from translation initiation to elongation. Nat Struct Mol Biol 2013; 20:150–8; PMID:23262488; http://dx.doi.org/10.1038/nsmb.2465

30. Pestova TV, de Breyne S, Pisarev AV, Abaeva IS, Hellen CUT. eIF2-dependent and eIF2-independent modes of initiation on the CSFV IRES: a common role of domain II. EMBO J 2008; 27:1060–72; PMID:18337746; http://dx.doi.org/10.1038/emboj.2008.49

31. Yamamoto H, Unbehaun A, Loerke J, Behrmann E, Collier M, Bürger J,Mielke T, Spahn CMT. Structure of the mammalian 80S initiation complex with initiation factor 5B on HCV-IRES RNA. Nat. Struct. Mol. Biol 2014; 21:721–7; PMID:25064512

32. Dibrov SM, McLean J, Parsons J, Hermann T. Self-assembling RNA square. Proc Natl Acad Sci USA 2011; 108:6405–8; PMID:21464284; http://dx.doi.org/10.1073/pnas.1017999108

33. Yu J, Liu Z, Jiang W, Wang G, Mao C. De novo design of an RNA tile that self-assembles into a homo-octameric nanoprism. Nat Commun 2015; 6:5724; PMID:25635537; http://dx.doi.org/10.1038/ncomms6724